

RC MODEL FOR CALCULATING THE SENSIBLE ENERGY DEMANDS IN BUILDINGS: ISO 52016-1 COMPARISON

Edwin S. Pinto^{1*}, Beatriz Amante
¹Polytechnic University of Catalonia, Barcelona, Spain

*Corresponding Author: edwin.samir.pinto@upc.edu

ABSTRACT

The energy consumption of the building sector has an important impact in the global energy demand and hence on the CO₂ emissions. Therefore, good strategies on the energy efficiency performance should be carried out, so it is important determine the thermal behaviour of the building. To this end, a grey box has been applied by using RC (Resistance-Capacitance) analogy to model the different components of the building envelope. The cases 600 and 900 presented in the ISO standard 52016-1:2017 were evaluated in order to validate the developed model. Based on the RC model, a state space model was set and solved by using *Simulink*. The results show a good match with respect to the ISO standard data, following the thermal dynamic behaviour of the building in both cases. The highest error in the indoor temperature was about 7% whereas errors up to 11% and 22% in the heating and cooling loads respectively were obtained. Therefore, further analysis should be carried out to achieve better results by improving the HVAC (Heating, Ventilation and Air Conditioning) system control.

1 INTRODUCTION

Despite the concern of the mankind regarding the climate change, the global net anthropogenic GHG (Greenhouse Gases) emissions have continued to rise during the period 2010-2019. In 2019 they were about 12% (6.5 GtCO₂eq) higher than in 2010 and 54% (21 GtCO₂eq) higher than in 1990 (Shukla et al., 2022). Among the global GHG emissions, the building sector reached 12 GtCO₂eq in 2019, equivalent to 21% of the global GHG emissions that year (Cabeza et al., 2022). This data shows the relevance of the building sector for achieving the global environmental goals. The environmental impact is linked to the energy consumption. In this respect, global final energy demand from buildings reached 128.8 EJ in 2019, and global electricity demand was slightly above 43 EJ. The former accounted for 31% of global final energy demand and the latter for 18% of global electricity demand. Among the building sector, residential buildings consumed 70% of global final energy demand from buildings (Cabeza et al., 2022). In this sense, retrofitting of existing buildings offers significant opportunities for reducing global energy consumption and greenhouse gas emissions (Ma et al., 2012). Therefore, the EU has established a legislative framework to boost the Energy Performance of Buildings. This updated framework includes, among others, the modernisation of the existing building stock and their systems, and better energy system integration (European Commission, 2021). Active and passive measures can be applied to improve the building energy performance. The former consists of the different energy supply technologies which enable the use of energy with a lower environmental impact (Pina, 2019; Pinto & Amante, 2022; Pinto Maquilon, 2021) and the latter are related to the improvement of the building envelope (Park et al., 2020; Thomas et al., 2018). However, in order to take actions on the buildings for retrofitting, it is important to know the energy demands of the buildings, actually, this could be considered the starting point of the retrofitting process. Therefore, it is required to develop building energy models to estimate their energy demands, but also for the control and optimization of the building energy system. There are three fundamental modelling techniques for building energy models namely black-box, white-box and grey-box (Li et al., 2021): i) The white-box model is fundamentally based on the physical laws. The common approach of making a white-box model is bottom-up (forward). The modelling is time-consuming due to many more required model parameters, but the simulation results are more accurate than other models. ii) The black-box model is a data-driven based modelling approach because of the boosting of machine learning algorithms. The typical

requirements for a black-box model are sufficient clean data and appropriate algorithms. It has multiple advantages, including lower engineering cost because it is a data-in-data-out approach; less domain knowledge because it is based on the mapping of input and output data; and greater adaptability because the model will evolve itself with new data. However, they also have some drawbacks, including a high demand for data quality, lack interpretability and may require intense computation especially with deep learning-based algorithms. iii) The grey-box model has the qualities of both white-box and black-box models. Grey-box models are sometimes called reduced-order models or simplified models. The grey-box model is more interpretable than black-box model. It is more computationally efficient and simpler than the white-box model.

Therefore, this work aims to develop a simple procedure including a simplified grey-box model based on resistance-capacitance (RC) system that allow the estimation of building energy demands. Since one of the crucial points for the computational models developing is the validation of the results, the ISO Standard 52016-1:2017 has been used for the validation. This work starts for the methodology description which includes the mathematical RC model and a brief description of the ISO standard to compare. The RC model is solved by using *Simulink* (The MathWorks Inc., 2022) and the results are compared with ISO standard data. Finally, some conclusions are presented focused on potential improvements.

2 METHODOLOGY

An RC model is developed to estimate the heating and cooling demands of a building (In this work, the term *building* is used regardless the number of zones, in this particular case, similar to the Standard 52016-1:2017, it refers of a single zone). The envelope is mainly composed of walls, windows, roof and floor. Each component is modelled based on a physical approach. However, some assumptions and limitations have to be considered for the RC models. Some of them are listed as follows (Li et al., 2021):

- Uniform zone temperature distribution or well-mixed zones is usually assumed.
- Long wave radiation between surfaces is ignored.
- Internal water vapor generation and heat transfer are neglected.
- Convective internal loads are treated as constant or slowly varying.
- Special boundary conditions are considered for heat transfer from floors and ceilings.
- Solar transmissivity is zero for opaque constructions.
- Windows are treated as pure resistances.

On the other hand, RC models have also some theoretical limitations such as:

- RC models do not handle the energy exchange between the return air and supply air well.
- Infiltration is not well modelled.
- The complexity will significantly increase with the number of zones for RC models. This will lead to intense computation burdens. Thus, model order reduction techniques are needed.

Nonetheless, the RC models, as grey-boxes, enable the representation of physical models with the advantage of having more flexibility for the analysis and the option to combine experimental data and physical modelling.

2.1 RC modelling for building envelope

There are different representations of RC models according to the literature. They are usually formatted into $xRyC$, in which x is the number of thermal resistances R , and y is the number of thermal capacitances C (Li et al., 2021). The Figure 1 shows different components representations of the building and their respective RC model. For instance, windows are usually modelled as $1R0C$ (Figure 1a). On the other hand, the walls can have as much layers as required. Each layer has a resistance and capacitance (Figure 1b). However, depending on the class of construction with respect to the

distribution of the mass in the construction, the capacitance can be distributed or concentrated (ISO, 2017). In this study, the mass of the layers is modelled concentrated in two points: internal and external (Figure 1c). Roof and floors are modelled similar to walls but considering that they have different boundary conditions.

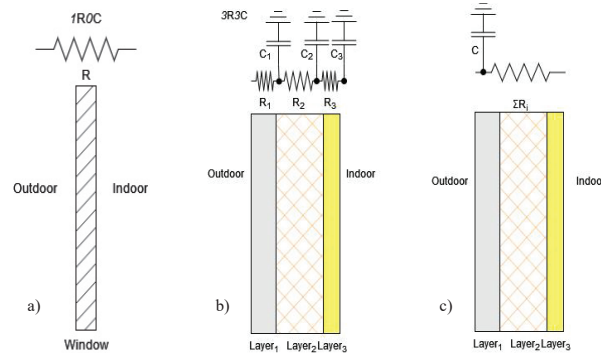


Figure 1: Usual RC model for a) Window; b) Wall; c) Simplified Wall.

Besides the envelope components, there are different physical aspects to be considered for modelling the building properly such as:

- The zone air is assumed to be well mixed and uniform. Along with the furniture, they are modelled with a single capacitor C_{in} .
- Indoor and outdoor convective/radiation resistances R_{in} and R_{out} respectively.
- Internal heat gains such as zone occupant heat gains, electrical equipment, and lighting Q_{ig} . Typically, they are represented as an ideal, single lumped parameter. Solar radiation transmitted through windows could also be included in the heat gains and treated as a lumped parameter.
- The infiltration is the flow into a zone through openings/cracks in the envelope from outside of the zone. They are usually assumed to be a disturbance or a lumped parameter Q_{inf} .
- The supplied energy to maintain the set temperature T_{set} is represented as a lumped parameter Q_{HVAC} . In other words, it is the thermal load to be calculated. This is represented in the Figure 2. The conditioned space at temperature T_{in} is the result of the energy balance of the gains Q_{gain} and loss Q_{loss} energy. To achieve and maintain the set temperature T_{set} defined by the user, an amount of energy Q_{HVAC} must be supplied/extracted from the space.

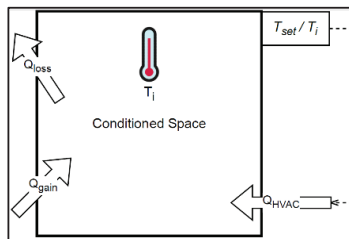


Figure 2: Representation of the thermal loads by calculating the HVAC (Heating, Ventilation and Air Conditioning) heating/cooling supply.

Additional aspects could be considered depending on the required modelling resolution. However, for the estimation of sensible loads, the aforementioned parameters are the most relevant. The Figure 3 shows the RC model representation for the main components of the building envelope. The general RC model could be tailored according to the analyzed component and their respective boundary conditions.

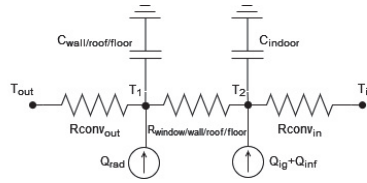


Figure 3: General RC model representation for the main components of the building envelope.

2.2 Mathematical solution of the RC model

This work aims to calculate the sensible thermal load of a building. Therefore, the main variable to calculate is the Q_{HVAC}. The Figure 4 depicts the heat flows in the general RC model representation. There are two heat flows sources Q₁ and Q₂ representing the set of lumped parameters described above.

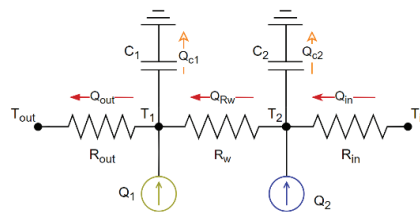


Figure 4: Heat flows in the general RC model.

The *nodal analysis method* is used to solve the RC model. This method states that the sum of currents in a node of the circuit must be zero. In thermodynamic words, it is carried out an energy balance in each node T₁, T₂ and T_{in} as follows:

$$\sum_{j=1}^n Q_j = 0 \tag{1}$$

Where Q_j represents the heats flows through the node. Following the electrical analogy, the heat flow through the resistance and capacitors can be expressed as:

$$\text{Resistance: } Q_R = \frac{\Delta T}{R} \tag{2}$$

$$\text{Capacitor: } Q_C = C \cdot \frac{dT}{dt} \tag{3}$$

Although the RC model for the envelope component is 1-D dimensional model (Figure 3), the building envelope is a 3-D dimensional analysis which include all the components (Figure 5). Therefore, the energy balance has to include the walls and windows in every direction as well as roof and floors.

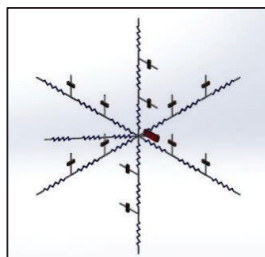


Figure 5: 3-D RC envelope model.

On the other hand, note that there are 2 nodes T_1 , T_2 for each envelope component and one common node T_{in} , which connect every RC model component. Therefore, based on the general RC model (Figure 4), the equations 2 and 3 are replaced in the equation 1 in each node to obtain:

$$\text{Node } T_1: Q_1 + \frac{T_2 - T_1}{R_W} - \frac{T_1 - T_{out}}{R_{out}} - C_1 \cdot \frac{dT_1}{dt} = 0 \quad (4)$$

$$\text{Node } T_2: \frac{T_{in} - T_2}{R_{in}} - \frac{T_2 - T_1}{R_W} - C_2 \cdot \frac{dT_2}{dt} = 0 \quad (5)$$

The subscript w represents any envelope component namely wall, window, roof or floor. The node T_{in} is common for every component:

$$\text{Node } T_{in}: Q_2 - C_{in} \cdot \frac{dT_{in}}{dt} - \sum_{\text{Component}} \frac{T_{in} - T_2}{R_{in}} = 0 \quad (6)$$

According to the International Standard (ISO, 2017): "The internal temperature of a building thermal zone is solved, on an hourly basis, by a system of equations of the transient heat transfers between the external and internal environment through the opaque and transparent elements bounding the zone's envelope. The equations are solved as a matrix. The calculation result is the temperature of each component, including the internal air and (if any) the heating or cooling needs". Therefore, the development of the above-mentioned equations for every component leads to a equation system that can be solved by *Simulink* (The MathWorks Inc., 2022) expressing the system in matrix form as:

$$\begin{aligned} E \cdot x' &= A \cdot x + B \cdot u \\ y &= C \cdot x + D \cdot u \end{aligned} \quad (7)$$

Where E is the mass matrix of the system, x is the state vector, u is the input vector, and y is the output vector. Matrix A , B , C and D are the state-space matrix. The dimensions of the matrix are: E [$N_x \times N_x$], A [$N_x \times N_x$], B [$N_x \times N_u$], C [$N_y \times N_x$], D [$N_y \times N_u$].

Different variables are involved in the model, 21 in total; however, depending of the required output for the analysis, it is determined the value y . For instance, if only the indoor temperature is required, the size of the different vectors and matrix are: E [21×21], A [21×21], B [21×8], C [1×21], D [1×8].

Defined the state-space model (SSM), it proceeds to set the *Simulink* model based on the objective of this work: To estimate the energy demands (heating and cooling) of a building. It proceeds to set the input parameters, matrix E , A , B and D . The elements of the matrices include mainly area, specific heat capacity and resistances. Matrix E is a diagonal matrix with the area and heat capacity of each element of the building affecting the transient behaviour. Matrix A is made up of different resistances parameters by conduction and convection/radiation. Matrix B includes different parameters in accordance with the input data vector u . This latter includes the outdoor temperature, solar radiation on different planes direction, and the heat gains. Besides, the HVAC system is included in a closed loop control. The Figure 6 shows the simplified *Simulink* layout of the RC model.

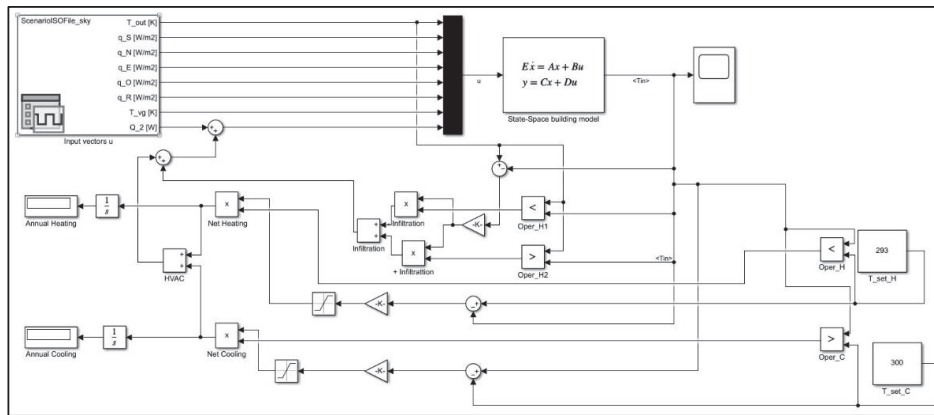


Figure 6. Simplified RC model Simulink layout

2.3 Model verification based on ISO 52016-1:2017

Verification cases described in the ISO 52016-1:2017 are used to evaluate and validate the developed RC model. The cases verify the calculation of the thermal balance in a single thermal zone and the calculation of the heating and cooling needs (ISO, 2017). The Figure 7 shows the test room used for the verification.

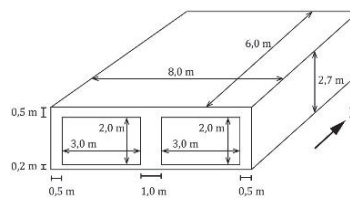


Figure 7: Geometry of the Test room.

Two verification cases are presented in this study: lightweight and heavyweight cases in continuous operation. They are labelled in the ISO standard as cases 600 and 900 respectively. Therefore, using the data of the ISO standard in the developed model, it is expected to obtain the same (or similar) results as those obtained in each case in the standard. This could be considered a theoretical validation of the model. Following, the different properties and parameters used for each case are presented. It is worthy to say that thermal bridges effect is not included in this test. Note that it is following the Standard procedure, besides, for the thermal bridge's analysis could be required more detailed information or a more complex test case that is out of the scope of this Standard test case.

2.3.1 Envelope properties

The Table 1 and Table 2 present the thermophysical properties of the opaque components namely walls, roof and floor for the lightweight and heavyweight cases respectively. Note that the specific heat capacity C is in $Wh/(m^2 \cdot K)$ because the time step used for the simulation is 1 hour. So, the original data in the standard in $J/(m^2 \cdot K)$ have been divided by 3600 to fit the units properly.

Table 1: Thermophysical properties of the opaque components for the lightweight case.

Structure	R [$W/(m^2 \cdot K)$]	C [$Wh/(m^2 \cdot K)$]
<i>External wall (Inside to outside)</i>		
Plasterboard	0,075	2,66
Fiberglass quilt	1,650	0,185
Wood siding	0,064	1,193

<i>Total surf-surf</i>	1,789	4,04
Floor (inside to outside)		
Timber flooring	0,179	5,417
Insulation	25,075	0
<i>Total surf-surf</i>	25,254	5,417
Roof (inside to outside)		
Plasterboard	0,063	2,217
Fiberglass quilt	2,795	0,313
Roofdeck	0,136	2,518
<i>Total surf-surf</i>	2,993	5,05

Table 2: Thermophysical properties of the opaque components for the heavyweight case.

Structure	R [W/(m ² ·K)]	C [Wh/(m ² ·K)]
External wall (Inside to outside)		
Concrete block	0,196	38,89
Foam Insulation	1,538	0,239
Wood siding	0,064	1,193
<i>Total surf-surf</i>	1,798	40,32
Floor (inside to outside)		
Concrete slab	0,071	31,111
Insulation	25,175	0
<i>Total surf-surf</i>	25,246	31,11
Roof (inside to outside)		
Plasterboard	0,063	2,217
Fiberglass quilt	2,795	0,313
Roofdeck	0,136	2,518
<i>Total surf-surf</i>	2,993	5,05

The windows consist of double pane glazing. The values of the resistance and transmittance are 0.335 m²·K /W and 0.71 respectively. In accordance with the ISO standard, capacitance and solar absorption are neglected.

Regarding the ground, for the application of the verification cases, it is assumed that the ground temperature is equal to the external air temperature. On the other hand, for the indoor air and furniture, the heat capacity shall be 2.78 Wh/(m²·K).

2.3.2 Heat transfer coefficients

The properties of the envelope determine the heat transfer mechanism by conduction. However, convection and radiation mechanisms are also involved in the model. These are proportional to the convective and radiation heat transfer coefficients. According to the ISO standard, the internal convective coefficient is different depending on the heat flow direction. However, for simplicity average values are considered in this study. Thus, the indoor and outdoor combined thermal resistance are 0.127 and 0.041 m²·K/W respectively.

2.3.3 Other thermal considerations

Outdoor radiation effect, internal gains and infiltration are also considered in the model. The former is calculated by applying a view factor of 1 and 0.5 for the roof and walls respectively, and an average difference between the apparent sky temperature and the air temperature of 11 K constant through the year. In the case of the internal gains and infiltrations, it is assumed an internal heat flow rate of 200 W and an air flow of about 53.3 m³/h respectively.

2.3.4 Thermostat control strategy

In order to estimate the heating and cooling loads, a continuous control strategy is applied for the verification cases. To this end, it is defined a set temperature for heating $T_{set,H}=20\text{ }^{\circ}\text{C}$ and for cooling $T_{set,C}=27\text{ }^{\circ}\text{C}$. The maximum available heating and cooling capacity ($Q_{HVAC,av}$) is effectively infinite, however in this work, this value is set in accordance to the HVAC mode to validate the model.

3 RESULTS

Aforementioned, two cases are used to validate the proposed model. These are the lightweight (case 600) and heavy case (case 900). Based on the available ISO standard results, the output data to compare are presented as follows:

1. Free floating (FF) temperature for January 4. This means the operative indoor temperature without any HVAC system.
2. Monthly and annual heating and cooling loads.
3. Peak heating and cooling demands.
4. Heating and cooling load hourly for January 4.

It is worthy to highlight that some mistakes have been found in the ISO standard 52016-1:2017. Some of them have been published by the EPB Center (Consultancy Service in the Energy Performance of the Building) (Dijk, 2022). In particular, we have taken into account the correct values of the monthly heating and cooling demands for the case 900 presented in the report (Dijk, 2022), instead of the wrong values presented in the tables 28 and 29 page 131 of the ISO Standard 52016-1:2017 (ISO, 2017).

3.1 Free floating temperature for January 4

The Figure 8 shows the dynamic behaviour of the building comparing the results obtained from the space state model (SSM) with respect to the ISO standard data. In both cases the space case model follows the dynamic behaviour presented in the ISO standard, however, it is observed an apparent delay

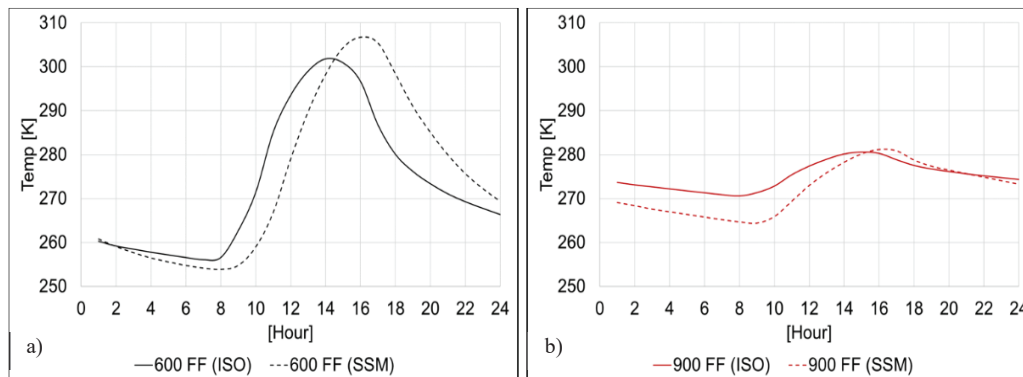


Figure 8: Indoor temperature behaviour without any HVAC system: a) Case 600 b) Case 900.

of about 1 hour approximately. The higher temperature difference in the case 600 occurs at 18 hours corresponding to at 7% approximately (Figure 8a). On the other hand, for the case 900 the higher difference occurs at 9 hours with an error of about 3% (Figure 8b).

The minimum and maximum temperatures are presented in Table 3. In both cases the maximum and minimum temperatures present a good match with errors below of 3%.

Table 3: Minimum and maximum temperatures in free floating mode.

	600 FF (SSM)	600 FF (ISO)	Error	900 FF (SSM)	900 FF (ISO)	Error
Max Temperature [K]	344	337	2,2%	322	317	-1,4%
Min Temperature [K]	255	253	0,8%	265	271	2,1%

3.2 Heating and cooling loads

To determinate the heating and cooling loads is one of the main objectives of the ISO standard 52016-1:2017. Likely, the *Simulink* model developed must be able to calculate the energy demands of the building. A HVAC control system is implemented in the model following the ISO standard guidelines. This could be considered an iterative process, since for the validation process, the values should match as much as possible the total annual energy loads presented in the ISO standard.

Therefore, the HVAC system supply the energy following the expression:

$$Q_{HVAC} = K_p \cdot \frac{T_{set} - T_{op,in}}{T_{HVAC} - T_{op,in}} \tag{8}$$

Where $T_{op,in}$ is the operative indoor temperature and T_{set} is the indoor set temperature. The constants K_p and T_{HVAC} are set according to the case and the HVAC mode.

3.2.1 Case 600

Applying an iterative process, the values of the K_p and T_{HVAC} are 30518 W and 280 K for heating, and 8719 W and 315 K for cooling. The Figure 9 shows the monthly heating and cooling loads for the case 600. The annual loads are about 1% above for both heating and cooling with respect to the ISO standard data. However, there are higher differences by month. For instance, for heating in July, the model calculates 15 kWh whereas the ISO standard only 6 kWh. Even so, in general terms, the model presents a good performance for both monthly heating and cooling demands.

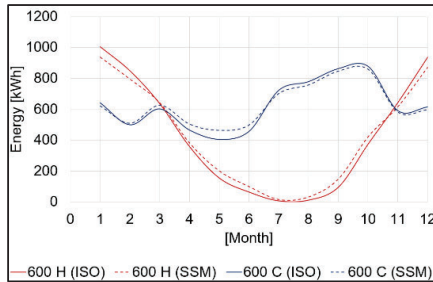


Figure 9: Monthly Heating and Cooling loads for case 600.

The peak heating and cooling demands are presented in the Table 4. In this case, the peak cooling load presents better results than peak heating loads with respect to the ISO standard data.

Table 4: Peak heating and cooling loads for case 600.

	(SSM)	(ISO)	Error
Heating [kWh]	3855	4351	-11.4%
Cooling [kWh]	6435	6363	1.1%

On the other hand, the Figure 10 shows the HVAC energy supply for the day January 4. The model follows the thermal dynamical behaviour quite similar to the ISO standard. The difference observed could be related with the offset observed in the free floating mode and due to the control system indeed.

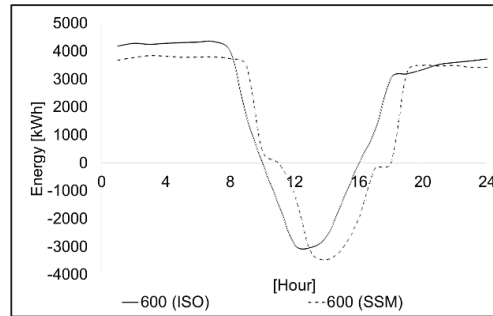


Figure 10: HVAC supply along January 4 for the case 600.

3.2.2 Case 900

Applying an iterative process, the values of the K_p and T_{HVAC} are 5232 W and 283 K for heating, and 3052 W and 312 K for cooling. The Figure 11 shows the monthly heating and cooling loads for the case 900. The annual loads are 0.3% and 0.9% above for heating and cooling respectively with respect to the ISO standard data. However, there are higher differences by month. For instances, for heating in September, the model calculates 11 kWh whereas the ISO standard only 1 kWh. Regarding Cooling loads, the model calculates 114 kWh in December whereas the ISO standard 48 kWh. In general terms, the model presents a good performance for monthly heating demands, whereas for cooling are observed significant mismatch.

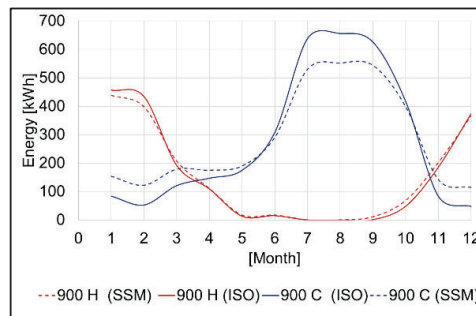


Figure 11: Monthly Heating and Cooling loads for case 900.

The peak heating and cooling demands are presented in the Table 5. Similar to the monthly energy loads results, the peak heating load calculated by the model presents a good match with the ISO standard. However, there is a significant mismatch in the peak cooling load value.

Table 5. Peak heating and cooling loads for case 900

	(SSM)	(ISO)	Error
Heating [kWh]	4064	4067	0.1 %
Cooling [kWh]	3295	4043	22.7 %

On the other hand, the Figure 12 shows the HVAC energy supply for the day January 4. The model follows the thermal dynamical behaviour until the hour 17. The HVAC system remains turned off 2 hours more than the ISO standard data. Similar to the previous case, it could be related with the offset observed in the free floating mode.

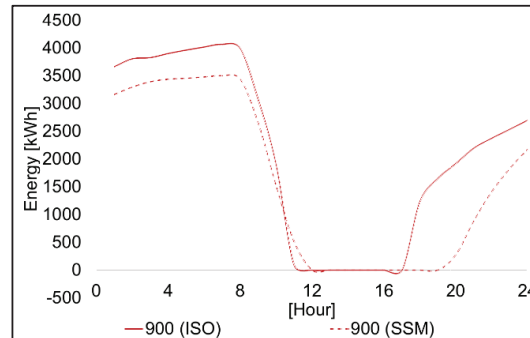


Figure 12: HVAC supply along January 4 for the case 900.

4 CONCLUSIONS

A grey box was developed to model the thermal performance of a building envelope by using Resistance-Capacitance (RC) analogy. A state space model was set based on the envelope building RC configuration. The solution was performed by using *Simulink*.

The validation of the developed model was carried out by evaluating the verification cases 600 and 900 presented in the ISO standard 52016-1:2017. According to the results, focused on the indoor temperature, the state space model follows the thermal behaviour of the envelope building with an apparent delay of 1 hour approximately. The highest error, about 7% is observed in the case 600, whereas the maximum error in the case 900 is about 3%.

Regarding the thermal loads, there is a good match in the monthly thermal performance with respect to the ISO standard data. However, significant differences are found in the months when lower HVAC supply is required.

Concerning the peak heating and cooling loads specifically, the former presents a significant difference with respect to the ISO standard data whereas the latter fits pretty well in the case 600 conversely to the case 900 where the peak heating load result are closest to the ISO standard in comparison to the peak cooling load result. Nonetheless, these results are subject to the iterative process carried to fit the annual heating and cooling loads. Besides, some assumptions such as the use of an average heat transfer coefficient could have affected the results. In general terms, for applications where the objective is to evaluate the tendency of the thermal behaviour of the building regarding the change of the different envelope properties, the grey box model developed could be considered as a reasonable tool, however, further research is required to understand the mismatches found in this study with respect to ISO standard, specially for the calculation of the heating and cooling loads.

REFERENCES

- Cabeza, L. F., Bai, Q., Bertoldi, P., Kihila, J. M., Lucena, A. F. P., Mata, É., Mirasgedis, S., Novikova, A., & Saheb, Y. (2022). *Buildings*. In *IPCC, 2022: Climate Change 2022: Mitigation of Climate Change*.
- Dijk, D. van. (2022). *Collection of comments and suggestions on EPB Standard: EN ISO 52016-1:2017 Energy performance of buildings — Energy needs for heating and cooling, internal temperatures and sensible and latent heat loads — Part 1: Calculation procedures*.

- <https://epb.center/support/documents/iso-52016-1/>
 European Commission. (2021). *Energy performance of buildings directive*.
https://energy.ec.europa.eu/topics/energy-efficiency/energy-efficient-buildings/energy-performance-buildings-directive_en
- ISO. (2017). *Standard ISO 52016-1:2017. Energy performance of buildings - Energy needs for heating and cooling, internal temperatures and sensible and latent heat loads - Part 1: Calculation procedures*. ISO.
- Li, Y., O'Neill, Z., Zhang, L., Chen, J., Im, P., & DeGraw, J. (2021). Grey-box modeling and application for building energy simulations - A critical review. *Renewable and Sustainable Energy Reviews*, 146, 111174. <https://doi.org/https://doi.org/10.1016/j.rser.2021.111174>
- Ma, Z., Cooper, P., Daly, D., & Ledo, L. (2012). Existing building retrofits: Methodology and state-of-the-art. *Energy and Buildings*, 55, 889–902.
<https://doi.org/https://doi.org/10.1016/j.enbuild.2012.08.018>
- Park, J. H., Yun, B. Y., Chang, S. J., Wi, S., Jeon, J., & Kim, S. (2020). Impact of a passive retrofit shading system on educational building to improve thermal comfort and energy consumption. *Energy and Buildings*, 216, 109930. <https://doi.org/10.1016/j.enbuild.2020.109930>
- Pina, E. A. (2019). *Thermoeconomic and environmental synthesis and optimization of polygeneration systems supported with renewable energies and thermal energy storage applied to the residential-commercial sector*. Universidad de Zaragoza.
- Pinto, E. S., & Amante, B. (2022). Polygeneration system optimization for building energy system retrofit: A case of study for TR5 building of UPC-Terrassa. *Energy and Buildings*, 112375. <https://doi.org/10.1016/J.ENBUILD.2022.112375>
- Pinto Maquilon, E. S. (2021). *Thermoeconomic and environmental optimization of polygeneration systems for small-scale residential buildings integrating thermal and electric energy storage, renewable energy and legal restrictions*. Universidad de Zaragoza.
- Shukla, P. R., Skea, J., Slade, R., Al Khourdajie, A., Van Diemen, R., McCollum, D., Pathak, M., Some, S., Vyas, P., Fradera, R., Belkacemi, M., Hasija, A., Lisboa, G., Luz, S., & Malley, J. (2022). *Summary for Policymakers. In: Climate Change 2022: Mitigation of Climate Change. Contribution of Working Group III to the Sixth Assessment Report of the Intergovernmental Panel on Climate Change*. <https://doi.org/10.1017/9781009157926.001>
- The MathWorks Inc. (2022). *Simulation and Model-Based Design* (9.12.0.1975300 (R2022a)).
- Thomas, A., Menassa, C. C., & Kamat, V. R. (2018). A systems simulation framework to realize net-zero building energy retrofits. *Sustainable Cities and Society*, 41, 405–420.
<https://doi.org/10.1016/j.scs.2018.05.045>

ACKNOWLEDGEMENT

The authors thank to the ENMA project 2021 SGR 0026 funded by the Agència de Gestió d'Ajuts Universitaris i de Recerca (AGAUR), the Polytechnic University of Catalunya-BarcelonaTECH and the Llabor-UPC project 2022.